Effect of Platelet Length and Stochastic Morphology on Flexural Behavior of Prepreg Platelet Molded Composites

Siavash Sattar[1], Benjamin Beltran Laredo[1], Richard Larson[1], Sergey Kravchenko[2], Oleksandr G. Kravchenko[1]

[1]Old Dominion University, Norfolk, Virginia, USA

[2] The University of British Columbia, Vancouver, Canada

Prepreg platelet molding compound (PPMC) can be used to create structural grade material with a heterogeneous mesoscale morphology. The three-dimensional stress transfer between interacting platelets depends on the platelet morphology and defines the macroscopic response of PPMC composite. The present work considered various platelet length of the prepreg system IM7/8552 to study the effect of the platelet length on the flexural behavior of PPMC composite. A progressive failure, finite-element analysis was used to aid in understanding competing failure modes in PPMC and how those modes are affected by the platelet length. Experimental results of the flexural tests of the PPMC with different platelet length sizes were used to validate the modeling prediction. The experimental and modeling results revealed the nonlinear behavior of the flexural mechanical properties (modulus and strength) on the platelet length. To study the non-uniformity in platelet local orientation, two modeling approaches to generate the stochastic PPMC morphology in the virtual samples based on the assigned global fiber orientation distribution (FOD) were used, namely, (*i*) generating individual coupons with a specific FOD and (*ii*) generating a virtual plaque with the same FOD that was then used to create various coupons. The results indicated an optimal platelet length for flexural mechanical behavior due to complex interactions between various damage mechanisms and the stochastic FOD variability in the material.

Keywords: Discontinuous reinforcement; Molding compounds; Prepreg platelet; Flexural properties; Damage mechanics

1. INTRODUCTION

Prepreg platelet molded composite (PPMC) is a material system processed by compression molding of unidirectional prepreg tape to achieve a discontinuous composite system with a heterogeneous mesoscale morphology, controlled fiber length, and 50–60% fiber volume fraction (FVF) [1]–[3]. PPMC structures are fabricated by cutting the prepreg tape into platelets with a prescribed length then compression molding the platelets into a required geometry (Fig.1) [3]. The collimated fibers of the same length within a platelet and the compression molding of the platelets results in enhanced mechanical properties and sufficient formability of PPMCs compared to the composites processed with sheet molding compound (SMC) or bulk molding compound (BMC) with 10-30% FVF [4], [5].

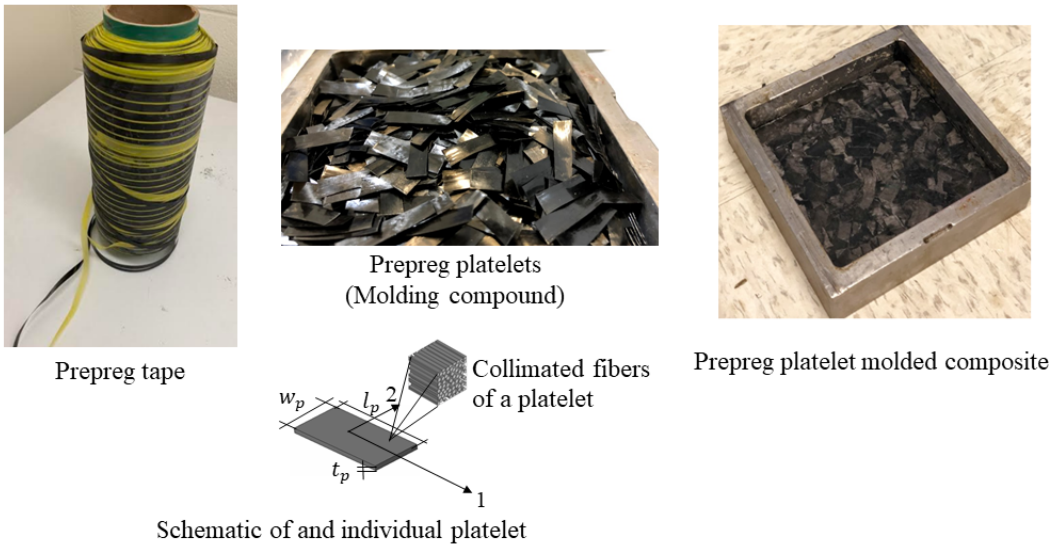

Fig.1 Prepreg platelet molded composite (PPMC) system

PPMC as a hierarchal composite system can be presented in two levels of length scale: (i) a micro-scale where individual fibers are distinguishable in a platelet, and (ii) a meso-scale, which includes the stochastic platelets distribution [6]. The stress transfer between the interacting platelets in the mesoscale defines the mechanical response of PPMCs. The local stress concentration occurred between the

platelets is a dominant factor that control the damage propagation and failure strength of PPMCs. The mesoscale stress transfer between the platelets in PPMCs depends on the composite mesostructure properties defined by the platelet geometrical parameters, orientation, and the number of the platelets [3]. The orientation state of PPMC describes how the platelets are oriented and is an important morphology descriptor in the PPMC meso-structure [2]. The orientation distribution of the platelets can be stochastic with irregular or deterministic with regular arrangement [6]. A stochastic distribution of PPMC is achieved when the orientation of the platelets results from the uncontrolled arrangement of the prepregs in the mold. The variability of the local structural platelet orientation and the non-symmetric distribution of local material properties results in the variation of the effective stiffness and strength of the material.

The main objective of this work is to develop a computational model to simulate and explain the variability of effective flexural modulus and strength of a stochastic PPMC and study the effect of the prepreg platelet length on the mechanical properties and failure mode. A continuum damage mechanism and a cohesive interfacial behavior was used to simulating the damage behavior and how the failure modes were affected by the platelet length. To study the effect of the platelet length on the flexural behavior of PPMC various platelet length, namely 1/4", 1/2” and 1” of the prepreg were considered. The proposed study is shown to support the experimental observation and can be used to investigate the structure-property relationship in PPMCs.

2. EXPERIMENTAL CHARACTERIZATION AND METHOD

The PPMC material system used for this study was a unidirectional Hexcel carbon fiber thermoplastic prepreg tape (IM7/8552). Three groups of coupons were fabricated with platelet length of 1/4", 1/2”, and 1” to study the effect of the platelet length on the distribution of the effective flexural properties of stochastic PPMC. The platelet width and thickness were 6.35 and 0.13 mm, respectively. The thickness and width of the fabricated coupons were 23 and 2.4mm, respectively. In the following sections, the microscopy analysis to calculate the platelet orientation state and the mechanical test procedure are outlined.

2.1.Microscopy analysis

The stochastic mesostructure of PPMCs is achieved by a random arrangement of the platelets in the mold following by an anisotropic flow of heterogeneous compound, results in a relocation and reorientation of the platelets [3]. A high-resolution microscopy analysis was used to measure the platelet orientation state in PPMCs with specified platelet length. Since the planar fiber orientation was assumed, the spatial orientation of fibers in each platelet was defined as the 2nd order symmetric tensor (Eq. 1) calculated as the dyadic product of the fiber orientation vector $\boldsymbol{p_i}$ (Eq. 2-3) based on the angle $\boldsymbol{\psi_i}$ between the plane's normal and the cylinder's longitudinal axis of the fiber. The angle of $\boldsymbol{\psi_i}$ is calculated by Eq. 4, where $\boldsymbol{l_i}$ and $\boldsymbol{h_i}$ are the major and minor diameter of the ellipse shape fiber, respectively. Eq. 5 was used to calculate the individual platelet orientation by taking the average over the calculated fibers orientation in the platelet, where $\boldsymbol{n_f}$ is the number of the fibers within the platelet. The global platelet orientation was measured by taking the average over the calculated individual platelet orientations (Eq. 6) where n_p is the number of the platelets [7], [8].

$$A_{ij\_fiber} = \begin{bmatrix} a_{11} & a_{12} \\ a_{21} & a_{22} \end{bmatrix} \tag{1}$$

$$a_{ij} = p_i p_j \tag{2}$$

$$p_i = \begin{bmatrix} cos\psi_i \\ sin\psi_i \end{bmatrix} \tag{3}$$

$$\psi_i = \text{acos}\,(h_i/l_i) \tag{4}$$

$$A_{ij\_platelet} = \frac{\sum_n A_{ij}}{n_f} \tag{5}$$

$$A_{ij\_Global} = \frac{\sum_n A_{ij\_platelet}}{n_p} \tag{6}$$

2.2 Mechanical testing

The effective flexural modulus and strength of stochastic PPMC coupons were measure in a displacement-control three-point bend tests with the span of 90mm using the MTS test machine with a 10kN load cell and with crosshead rate of 2 mm. Flexural stress and strain stress were calculated through equations 7 and 8, respectively, where, *F* is the applied load, *L* is the span length, *b* is the width of the specimen, *t* is the thickness and *d* is the deflection. Fig.2 shows three-point bending setup with 90 mm span for a PPMC sample.

$$\sigma = \frac{3FL}{2bt^2} \tag{7}$$

$$\varepsilon = \frac{6tD}{L^2} \tag{8}$$

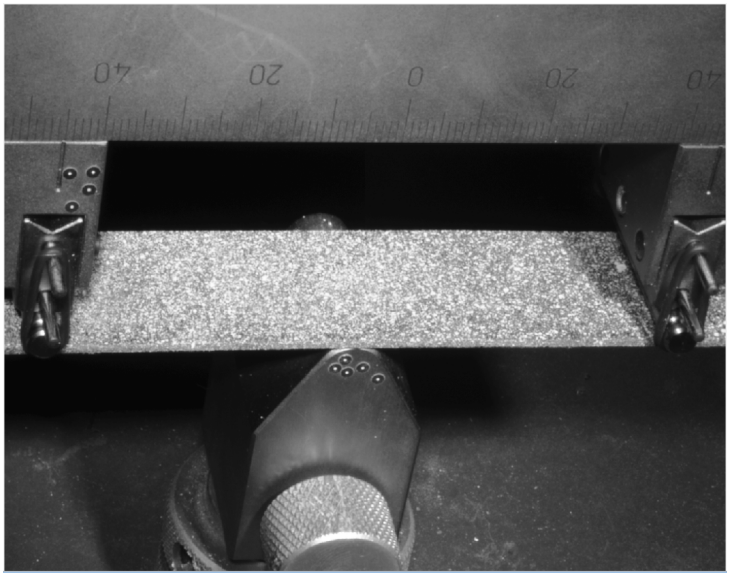

Fig2. three-point bending setup for a PPMC sample with 90 mm span

3. MODELING PROCEDURE FOR PROGRESSIVE FAILURE ANALYSIS

A 3D finite element computational model with the damage mechanism approach was developed to simulate the three-point bending test using Abaqus implicit and predict the flexural modulus and strength of the PPMCs as well as the failure mode. The mesostructure of virtual PPMC is generated in DIGIMAT FE including 100% of platelets using probabilistic modeling to predict the statistical distributions of effective flexural properties of stochastic PPMCs [9]. The validation of the probabilistic simulation results is based on the comparison between experimental and predicted

distributions using analysis of variance by the two-sample t-test to test for statistical significance. The two-sample tests is a statistical test used to determine if the two samples population means are equal at the certain significance level. The difference between the sample distribution is statistically significant if the probability of the phenomenon (p-value) is less than 5% [10]. The following sections outlined the mesostructure generation of the virtual specimens and the damage mechanism used in the model.

3.1.Meso-structure generation and virtual flexural test setup

The stochastic structural arrangement of platelets is calculated through the sequential adsorption algorithm and in ta random placement the center of the platelets sequentially. Fig.3-a shows a virtual coupon with 1" prepreg platelet meso-structure. The platelets were generated within the voxel mesh by generating voxels into a platelet and assigning the local orientation vector (Fig3-c). The cohesive elements were generated at the interface of the platelets to define the interaction between them. Fig.3-d-e shows overlapping platelets including a cohesive interface and the schematic for the idealized stress components. The FVF of the platelets is equal to that of the parent tape and was included in the model by using characterized material properties for the prepreg tape to the platelets. Two approaches were used to generate the virtual morphology of the specimens, namely, (i) individual virtual coupons generated with the 2D random platelet orientation in a full-size flexural test specimen ($110 \times 25 \times 2.4mm$), and (ii) split coupons from a generated 5"×5" plaque with the random platelet orientation. After generation of the virtual specimens, the model is imported into Abaqus to apply three-point bending with boundary conditions and constitutive models for the platelets and their interfaces [11]. Fig.3-b shows a deformed state of 3-point bending model of a PPMC sample with 1" prepreg platelet length.

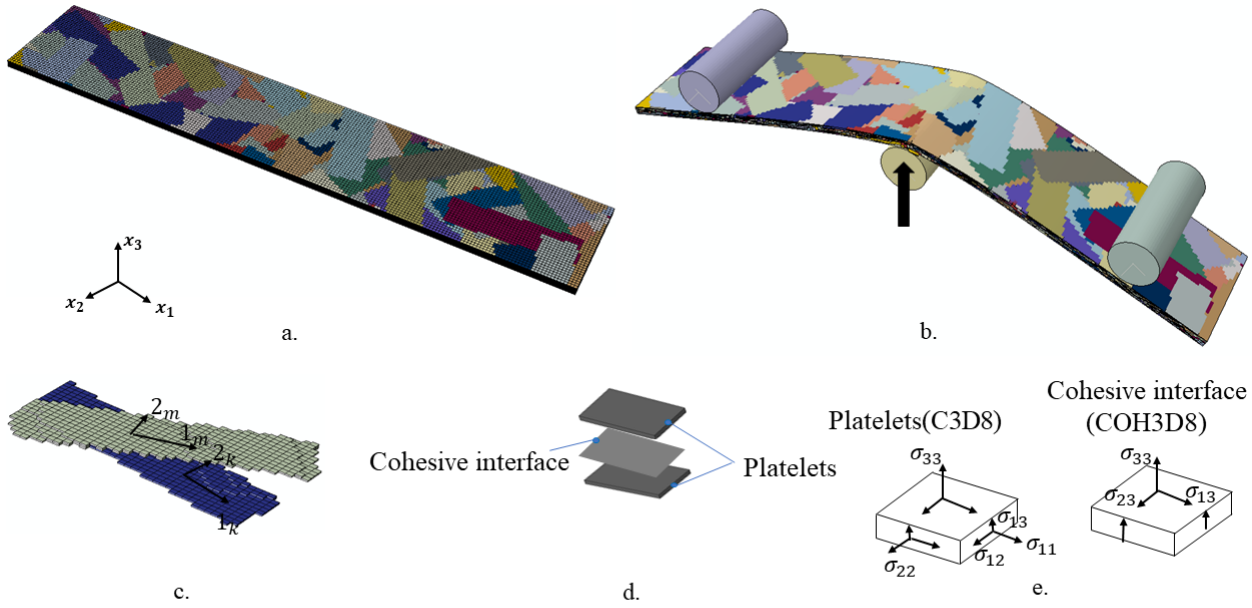

Fig. 3 a. A virtual coupon with prepreg platelet meso-structure; b. Deformed state of 3-point bending model c. Platelet fiber direction vectors in the global coordinate system d. Schematic of the overlapping of the platelets with cohesive element e. stress components on a platelet and cohesive element

3.2.Constitutive modeling of PPMCs

The individual platelets in meso-scaled computational model considered as a homogeneous orthotropic material with the properties of the parent UD prepreg tape. The continuum damage mechanics (CDM) with orthotropic damage for platelets combined with a cohesive zone modeling (CZM) at the interfaces between platelets to capture delamination.

A stiffness reduction scheme is used to describe the damaged response of the platelets using commercially available user subroutine UMAT [12]. The platelets assumed as an orthotropic homogenized material following constitutive relationship in Eq. 9, where C_{ij} is the damaged stiffness matrix depending on the virgin (undamaged) stiffness components (C_{ij}^{0}) and the state of the damage variables in the fiber direction (d_1) and transverse to the fiber direction (d_2). The damage stiffness components were computed through Eq. 10.

$$\begin{bmatrix}\sigma_{11}\\ \sigma_{22}\\ \sigma_{33}\\ \sigma_{12}\\ \sigma_{13}\\ \sigma_{23}\end{bmatrix} = \begin{bmatrix}C_{11} & C_{12} & C_{13} & 0 & 0 & 0\\ C_{12} & C_{22} & C_{23} & 0 & 0 & 0\\ C_{13} & C_{23} & C_{33} & 0 & 0 & 0\\ 0 & 0 & 0 & C_{44} & 0 & 0\\ 0 & 0 & 0 & 0 & C_{55} & 0\\ 0 & 0 & 0 & 0 & 0 & C_{66}\end{bmatrix} \times \begin{bmatrix}\varepsilon_{11}\\ \varepsilon_{22}\\ \varepsilon_{33}\\ \gamma_{12}\\ \gamma_{13}\\ \gamma_{23}\end{bmatrix} \quad (9)$$

$$C_{11} = (1-d_1)C_{11}^0 \ , \quad C_{12} = \left(1-d_1)(1-d_2)C_{12}^0 \right. \ , \quad (10)$$
$$C_{13} = \left(1-d_1)C_{13}^0 \right. ,$$
$$\left(1-d_2)C_{22}^0 \right. , C_{23} = C_{23}^0, C_{33} = C_{33}^0,$$
$$C_{44} = \left(1-d_1)(1-d_2)C_{44}^0 \right. , C_{55} = C_{55}^0 \ , C_{66} = C_{66}^0$$

The failure initiation criterion is predicted by applying the damage initiation functions f_1 and f_2 for damage variable d_1 and d_2, respectively (Eq.11 and 12).

$$f_1 = \sqrt{\frac{\varepsilon_{11}^2}{\varepsilon_{11}^{f,t}\varepsilon_{11}^{f,c}} + \varepsilon_{11} \times \left(\frac{1}{\varepsilon_{11}^{f,t}} - \frac{1}{\varepsilon_{11}^{f,c}}\right)} = 1 \quad (11)$$

$$f_2 = \sqrt{\frac{\varepsilon_{22}^2}{\varepsilon_{22}^{f,t}\varepsilon_{22}^{f,c}} + \varepsilon_{22} \times \left(\frac{1}{\varepsilon_{22}^{f,t}} - \frac{1}{\varepsilon_{22}^{f,c}}\right) + \left(\frac{\varepsilon_{12}}{\varepsilon_{12}^{f}}\right)^2} = 1 \quad (12)$$

where $\varepsilon_{ii}^{f,t}$ and $\varepsilon_{ii}^{f,c}$, (i=1, 2), are the failure strains in the in-plane principal directions in tension and compression, respectively; ε_{12}^{f}, is the failure strain in shear. The damage variable d_1 and d_2 are computed by Eq 13, where the damage variable evolves from 0 to 1 and l^* is the characteristic element length associated to the material, and $\boldsymbol{G_i^f}$ is the fracture energy.

$$d_i = 1 - \frac{\varepsilon_{\mathrm{ii}}^{f,t}}{f_{\mathrm{i}}} \exp\left(\frac{C_{\mathrm{ii}} \varepsilon_{\mathrm{ii}}^{f,t} \left(\varepsilon_{\mathrm{ii}}^{f,t} - f_{\mathrm{i}} \right) l^*}{G_i^f} \right), \; i = 1,2 \tag{13}$$

Delamination of platelets is modeled with cohesive zone mechanism using a traction separation law. Eq. 14 shows the constitutive equation law of traction separation where interlaminar σ_{ij} stress, δ_j is the relative separations between the elements, d is the damage variable, and $k_i^0 = 1 \times 10^6 \frac{MPa}{mm}$ is the initial stiffness [13].

$$\begin{bmatrix} \sigma_{13} \\ \sigma_{23} \\ \sigma_{33} \end{bmatrix} = \begin{bmatrix} (1-d)k_1^0 & 0 & 0 \\ 0 & (1-d)k_2^0 & 0 \\ 0 & 0 & (1-d)k_3^0 \end{bmatrix} \begin{bmatrix} \delta_1 \\ \delta_2 \\ \delta_3 \end{bmatrix} \tag{14}$$

The failure initiation criterion of the disbanding between the platelets are given by Eq. 15 where $N_{max} = 50MPa$ and $S_{max} = T_{max} = 80MPa$ are the cohesive strength.

$$\left(\frac{\sigma_{33}}{N_{max}}\right)^2 + \left(\frac{\sigma_{13}}{S_{max}}\right)^2 + \left(\frac{\sigma_{23}}{T_{max}}\right)^2 = 1 \tag{14}$$

The propagation of the delamination is defined by a linear fracture mechanism of power law through Eq. 15 [14].

$$\frac{G_I}{G_{IC}} + \frac{G_{II}}{G_{IIC}} + \frac{G_{III}}{G_{IIIC}} = 1 \tag{15}$$

where $G_I,\ G_{II},\ G_{III}$ are the work done by the tractions and their corresponding displacements in the normal and shear directions, and $G_{IC},\ G_{IIC},\ G_{IIIC}$ are the critical strain energy release rates corresponding to the fracture mode. The stiffness and strength properties of the orthotropic platelets of IM7/8552 prepreg tape were adopted from [15], [16].

4. RESULTS

4.1.Characterization of the local platelet orientation

The local platelet orientation state of PPMCs were measured for polished specimens using Eq. 1-6. Fig. 4 shows three cross-sectional images captured at a random location of polished samples fabricated with 1", ½", and ¼" prepreg platelet length. Longer platelet length in stochastic PPMCs means a smaller number of platelets in a specimen, resulting in fewer possible orientation states, a more non-uniform local platelet orientation, and loss of heterogeneity. This implies how the platelet size changes the orientation state and morphology of the entire system. The first component of the platelet orientation tensor, shown in Fig.4, is representative the platelet degree of alignments for each cross-sectional image. The local platelet orientation showed an aligned platelet orientation state at a specific location of the stochastic PPMC.

a.

$$A_{ij} = \begin{bmatrix} 0.22 & 0.41 \\ 0.41 & 0.78 \end{bmatrix}$$

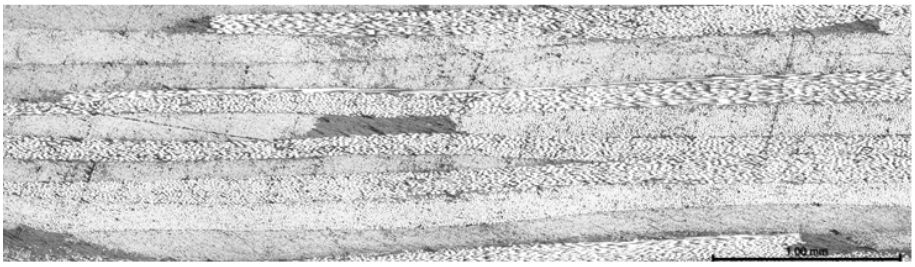

b.

$$A_{ij} = \begin{bmatrix} 0.27 & 0.44 \\ 0.44 & 0.73 \end{bmatrix}$$

c.

$$A_{ij} = \begin{bmatrix} 0.23 & 0.42 \\ 0.45 & 0.77 \end{bmatrix}$$

Fig.4 Cross-section micrographs of PPMCs with a. 1", b. ½", and c. ¼" prepreg platelet length

4.2.Comparison of experimental and numerical modeling prediction

The effective flexural modulus and strength of the PPMCs were measured through the experiments and compared with the simulation results. Figure 5 shows an example of predicted macroscopic stress–strain curves related to the virtual coupons with prepreg length of 1", ½", and ¼" compared to the stress-strain response from the three-point bending tests. The initial linear global response of the stress-strain behavior followed by a progressive global stiffness degradation leading to a non-linear stress-strain behavior before the ultimate strength was reached. A similar gradual decease of stress was observed in both simulations and experiments after reaching the maximum stress.

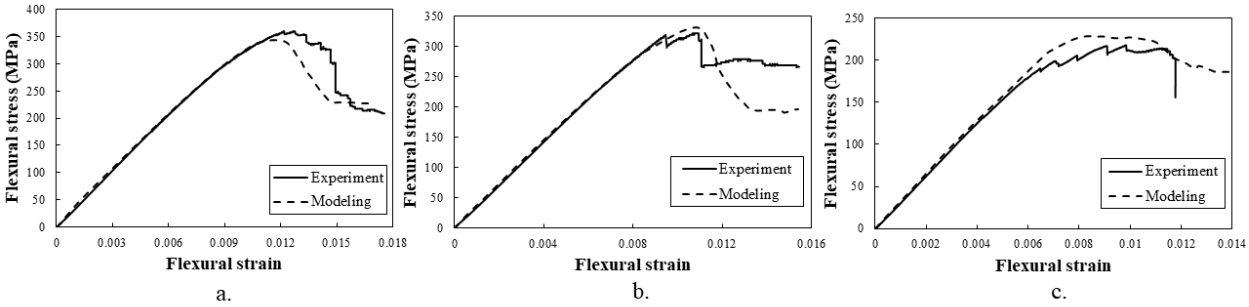

Fig. 5 Flexural stress strain behavior of the experiment and modeling of the PPMCs with a. 1", b. ½", and c. ¼" prepreg platelet length

Platelet length is an effective parameter in PPMCs to characterize the mesostructure and the mechanical properties of the material. Fig. 6 summarize the results of predicted effective flexural modulus and strength of PPMCs with platelet length of 1", 1/2", and 1/4" compared with the experiments. Two approaches were considered to generate the stochastic PPMC morphology of the virtual coupons with the 2D random orientation, namely, (approach1) generating individual coupons with the full size of specimen, (approach2) generating a virtual 5"×5" plaque that was then used to create various coupons. Validation of results of two simulation approach was performed by comparing the experimental and simulation property distributions by the two-sample t-test, wherein the null hypothesis stated that there is no difference between the distributions. The variation of the flexural modulus and strength, shown in Fig. 6, results from the variability of the local structural platelet orientation and the non-symmetric distribution of local material properties. The test results indicates that PPMCs with longer platelet length (1") shows a lower average flexural strength and modulus compared with PPMCs of ½" prepreg platelet length. Fewer number of platelets in a PPMC specimen with longer platelets leads to a more non-uniform local platelet orientation and the loss of stiffness and strength. Reducing the platelet length from 1/2" to ¼" in PPMCs results in decreasing the flexural modulus and strength of the material due to the reduced stress sharing between longer platelets. The simulation results for two approaches agreed with the test results and showed a decreasing trend of average flexural strength and modulus with reducing the platelet length from 1" to ¼". The p-value of the two-sample t-test between the predicted flexural strength and

modulus obtained from simulations and the flexural strength and modulus measured from the experiments are greater than 0.05. Therefore, the null hypothesis was not rejected, and two sample distributions are not significantly different at the 5%, implying that the simulation results for both approaches can be considered reliable.

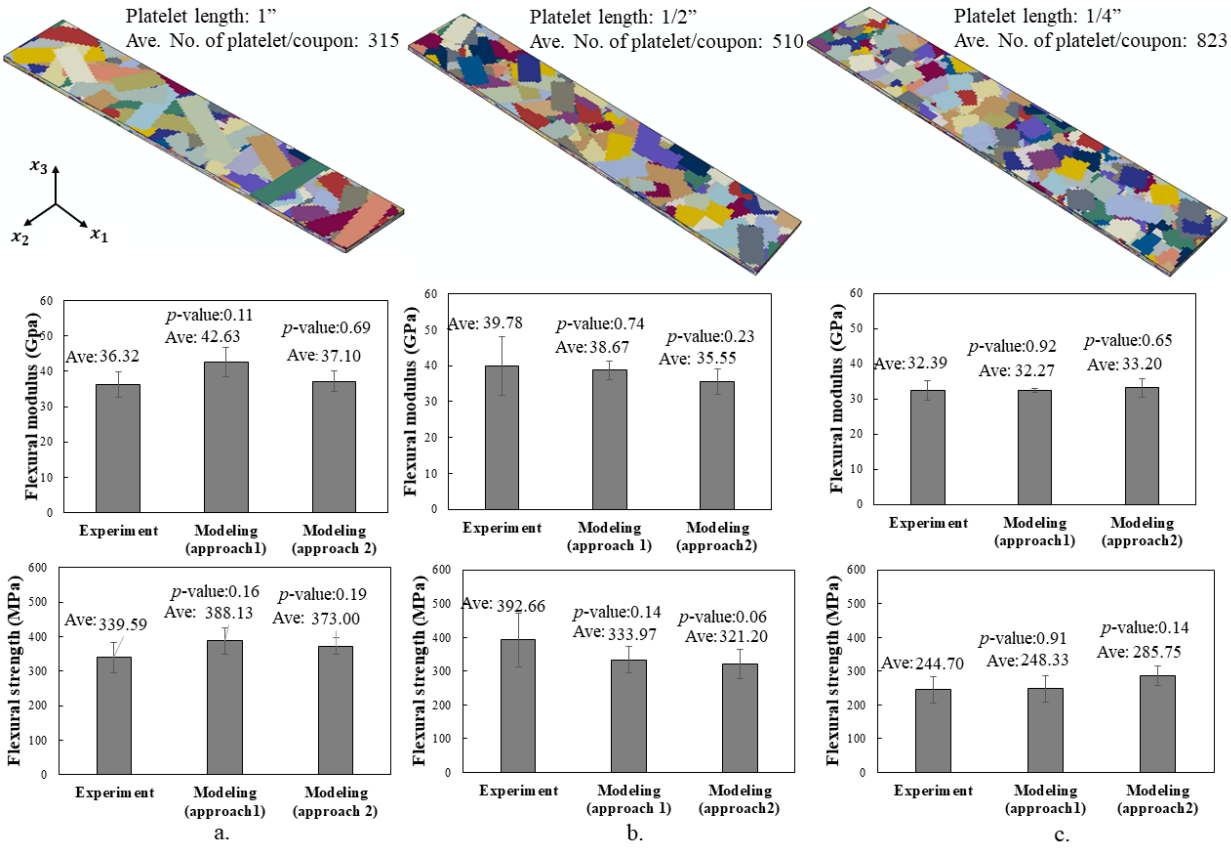

Fig.6 Variability of effective flexural modulus and strength in a stochastic PPMC made of a. 1”, b. ½”, and c. ¼” platelet length in simulations and experiments

4.3.Analysis of damage states

Figure 7 compares the cumulative relative frequency of the damage variables for the two selected virtual coupons in every batch of simulations of approach 2. S1 and S2 in Fig. 7 indicated the sample with maximum and minimum ultimate strength (shown in the legend) in every batch of PPMC modeling with prescribed platelet length. The pattern of the damage variable in the fiber direction, transverse to the fiber direction, and through the thickness is shown at the maximum stress for a selected virtual coupon with maximum ultimate strength in every batch of modeling with approach 2.

The damage variable through the thickness corresponds to the delamination of the platelets. The cumulative relative frequency of damage variables was calculated in damage process zone by considering the damaged elements as a fraction of total number of the elements. The damage was confined to the region of 20mm around the middle roller for all simulations, which was identified as the damage process zone (Figure 7). The distribution of the damage variables in damage process zone shows multiple local failures in the matrix direction and through the thickness. The cumulative frequency of different damage variables did not show a similar trend for two selected virtual coupons in correlation with the platelet length of PPMCs, implying the effect of the stochastic arrangement of platelets and the non-symmetric distribution of local material properties on the failure mode.

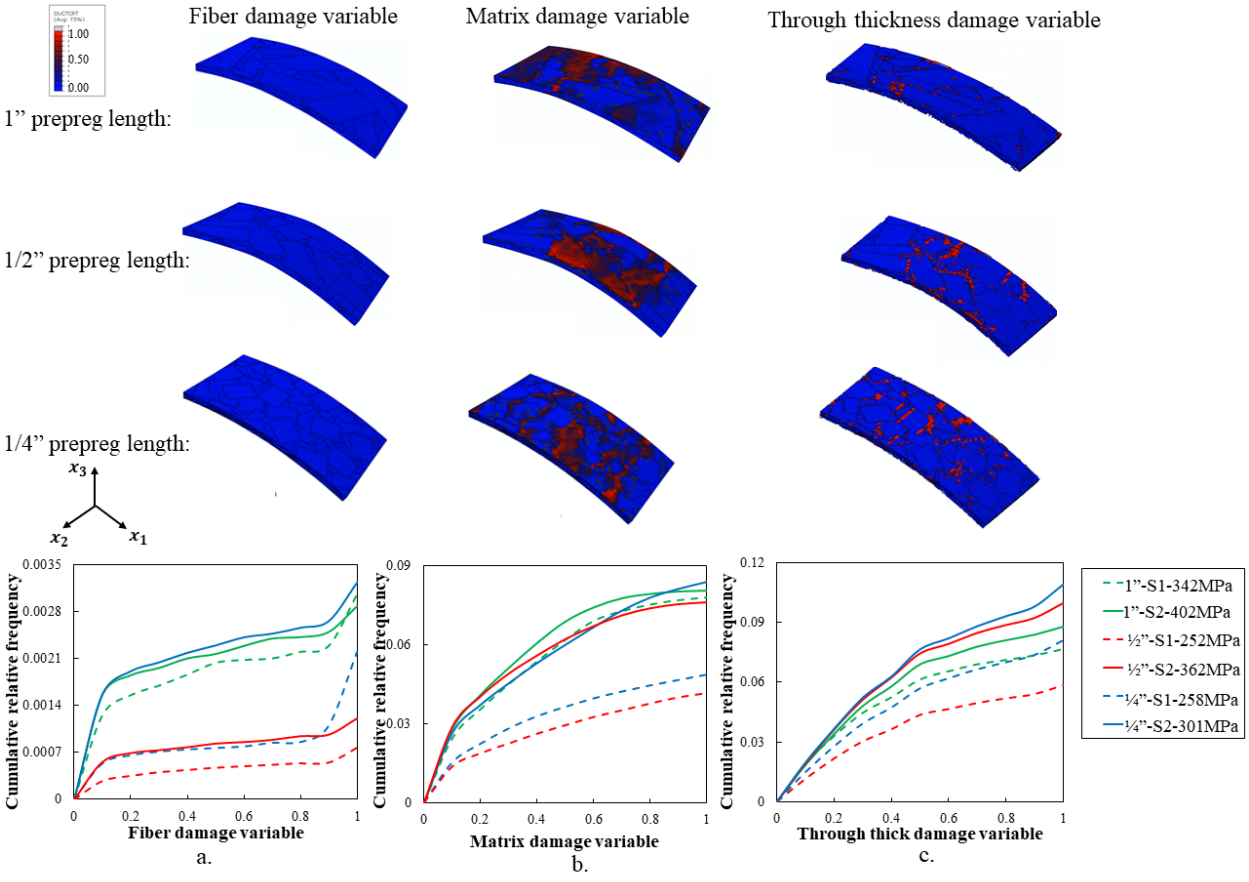

Fig. 7 Distribution and cumulative frequency of the damage variable in a. fiber direction, b. transverse to the fiber, and c. through the thickness in three-point bending simulations of PPMCs with 1", ½", and ¼" prepreg platelet length

5. CONCLUSION

In this study, a progressive failure analysis was used to study the effect of the prepreg platelet length of PPMCs with stochastic morphology on the flexural properties and the failure behavior of the material. A continuum damage mechanism was used for modeling the evolution of damage in the platelet meso-structure, coupling with a surface-based cohesive behavior implemented between the platelets to simulate the interfacial delamination. The variable mesostructur geometry of PPMCs leads to the variability of flexural modulus and strength. It was shown that the platelet length controls composite effective flexural modulus and strength. Longer platelet length leads to the enhanced stress sharing between the platelets Furthermore, fewer platelets in PPMCs with longer platelet length exhibit more dissimilarity in the meso-morphology and non-uniform local platelet orientation. Experimental studies showed that improved average flexural strength and modulus for the PPMCs with ½" platelet length compared with the PPMCs with 1" and ¼" platelet length. The variability of effective flexural properties caused by the variability of stochastic mesostructure is shown by simulation results. To validate the simulation results, the analysis of statistical significance of the difference between the probabilistic distributions of properties obtained from the simulations and experiments was analyzed through the Student's t-test. The simulation results showed that the dominant failure modes were the delamination between the platelets and the transverse failure in the platelets. The failure mechanism varied from one coupon to another due to the local morphological dissimilarities, specifically the local stochastic orientation state of the platelets. The developed stochastic progressive failure modeling for PPMCs can be used for predicting mechanical behavior and associated uncertainty in composite response resulting from the local platelet orientation state and platelet morphology.

References

[1] J. Aubry, "HexMC — bridging the gap between prepreg and SMC," *Reinforced Plastics*, vol. 45, no. 6, pp. 38–40, Jun. 2001, doi: 10.1016/S0034-3617(01)80207-1.

[2] S. G. Kravchenko, D. E. Sommer, B. R. Denos, W. B. Avery, and R. B. Pipes, "Structure-property relationship for a prepreg platelet molded composite with engineered meso-morphology," *Composite Structures*, vol. 210, pp. 430–445, Feb. 2019, doi: 10.1016/j.compstruct.2018.11.058.

[3] S. G. Kravchenko *et al.*, "Tensile properties of a stochastic prepreg platelet molded composite," *Composites Part A: Applied Science and Manufacturing*, vol. 124, p. 105507, Sep. 2019, doi: 10.1016/j.compositesa.2019.105507.

[4] P. Feraboli, E. Peitso, F. Deleo, T. Cleveland, and P. B. Stickler, "Characterization of Prepreg-Based Discontinuous Carbon Fiber/Epoxy Systems," *Journal of Reinforced Plastics and Composites*, vol. 28, no. 10, pp. 1191–1214, May 2009, doi: 10.1177/0731684408088883.

[5] I. Taketa, T. Okabe, H. Matsutani, and A. Kitano, "Flowability of unidirectionally arrayed chopped strands in compression molding," *Composites Part B: Engineering*, vol. 42, no. 6, pp. 1764–1769, Sep. 2011, doi: 10.1016/j.compositesb.2011.01.021.

[6] S. G. Kravchenko, D. E. Sommer, and R. B. Pipes, "Uniaxial strength of a composite array of overlaid and aligned prepreg platelets," *Composites Part A: Applied Science and Manufacturing*, vol. 109, pp. 31–47, Jun. 2018, doi: 10.1016/j.compositesa.2018.02.032.

[7] T. B. Nguyen Thi, M. Morioka, A. Yokoyama, S. Hamanaka, K. Yamashita, and C. Nonomura, "Measurement of fiber orientation distribution in injection-molded short-glass-fiber composites using X-ray computed tomography," *Journal of Materials Processing Technology*, vol. 219, pp. 1–9, May 2015, doi: 10.1016/j.jmatprotec.2014.11.048.

[8] R. S. Bay and C. L. Tucker, "Stereological measurement and error estimates for three-dimensional fiber orientation," *Polymer Engineering & Science*, vol. 32, no. 4, pp. 240–253, 1992, doi: 10.1002/pen.760320404.

[9] "Digimat User's Manual. Version 2017." e-Xstream Engineering. MSC.

[10] D. C. Montgomery, *Design and analysis of experiments*, Eighth edition. Hoboken, NJ: John Wiley & Sons, Inc, 2013.

[11] "Abaqus Analysis User's Guide (6.14)." http://130.149.89.49:2080/v6.14/books/usb/default.htm?startat=pt05ch23s06abm37.html (accessed Oct. 28, 2019).

[12] “Abaqus 2016 Documentation.” http://130.149.89.49:2080/v2016/index.html (accessed Jul. 18, 2021).

[13] P. Camanho and C. G. Davila, “Mixed-Mode Decohesion Finite Elements for the Simulation of Delamination in Composite Materials.” 2002.

[14] J. D. Whitcomb, *Analysis of Instability-related Growth of a Through-width Delamination*. National Aeronautics and Space Administration, Langley Research Center, 1984.

[15] T. N. Sti, T. T. Strength, T. K. Oõbrien, and R. Krueger, “Analysis of Ninety Degree Flexure Tests for Characterization of Composite U.S. Army Research Laboratory Vehicle Technology Directorate NASA Langley Research Center.” 2001.

[16] “Hexcel | Composite Materials and Structures.” https://www.hexcel.com/ (accessed Jul. 19, 2021).